Novel insertional presenilin 1 mutation causing Alzheimer disease with spastic paraparesis

P. Moretti, A. P. Lieberman, E. A. Wilde, B. I. Giordani, K. J. Kluin, R. A. Koeppe, S. Minoshima, D. E. Kuhl, W. K. Seltzer and N. L. Foster

Neurology 2004;62;1865-1868

Novel insertional presenilin 1 mutation causing Alzheimer disease with spastic paraparesis

P. Moretti, MD; A.P. Lieberman, MD; E.A. Wilde, PhD; B.I. Giordani, PhD; K.J. Kluin, MS; R.A. Koeppe, PhD; S. Minoshima, MD, PhD; D.E. Kuhl, MD; W.K. Seltzer, PhD; and N.L. Foster, MD

Abstract—A four-generation pedigree exhibiting early-onset autosomal dominant Alzheimer disease (AD) with spastic paraplegia, dystonia, and dysarthria due to a novel 6-nucleotide insertional mutation in exon 3 of the presenilin 1 gene (PS1) is described. Serial examinations, PET scans, and autopsy revealed that the mutation in this highly conserved portion of PS1 causes an aggressive dementia that maintains the usual regional hierarchy of disease pathology while extending abnormalities into more widespread brain areas than typically seen in AD.

NEUROLOGY 2004;62:1865–1868

Dementia with spastic paraparesis has been reported in several dominantly inherited neurologic conditions, including early-onset familial Alzheimer disease (AD), familial British dementia with amyloid angiopathy, hereditary spastic paraparesis (HSP), and Gerstmann–Straüssler–Scheinker syndrome. AD with spastic paraparesis is caused by presenilin 1 gene (*PS1*) mutations.[1,2] Early-onset AD with spastic paraparesis was originally reported at the University of Michigan in 1913.[3] We describe the clinical, metabolic, and pathologic characteristics of AD with spastic paraparesis due to a novel *PS1* mutation in an apparently unrelated Michigan family.

Methods. We examined two siblings with early-onset dementia (Cases IV.2 and IV.3) and obtained from family members information about members of three prior generations who had a similar illness.

PET with [^{18}F]fluoro-2-deoxy-D-glucose (FDG-PET) was performed in Cases IV.3 and IV.2. Metabolic changes in these subjects were compared with those of 27 patients with autopsy-confirmed AD, who had no known genetic mutation and varying degrees of dementia severity.[4-6] Additional comparisons were performed with FDG-PET results from 33 normal subjects.

Postmortem brain tissue was fixed in 10% formalin and processed for paraffin embedding and immunohistochemical analysis. Previously characterized antibodies against β-amyloid peptide (DAKO, Carpinteria, CA), tau (Sigma Chemical Co., St. Louis, MO), and glial fibrillary acidic protein (DAKO) were used according to the manufacturers' recommendation.

Additional material related to this article can be found on the *Neurology* Web site. Go to www.neurology.org and scroll down the Table of Contents for the May 25 issue to find the title link for this article.

Blood samples were taken from Cases IV.3 and IV.2 and their unaffected mother. Direct testing for mutations in the coding region of the *PS1* gene was performed at Athena Diagnostics, Inc. (Worchester, MA) by PCR amplification of genomic DNA and cDNA followed by automated sequencing of both DNA strands. The cDNA template for PCR was prepared by reverse transcription of *PS1* messenger RNA purified from blood lymphocytes.

Results. The proband's paternal great-grandfather (I.1), grandfather (II.3), and father (III.3) died in their thirties of a dementing illness associated with severe progressive gait impairment (see the pedigree in the supplementary material on the *Neurology* Web site; go to www.neurology.org).

The proband (IV.3) developed memory problems at age 28 years. By age 31, he had mild bilateral limb apraxia, left-hand dystonia, and brisk stretch reflexes in the lower extremities. His gait was normal. Initial neuropsychological testing showed mild dementia (table). Laboratory studies for reversible causes of dementia were normal, and brain MRI showed mild atrophy. FDG-PET demonstrated significant hypometabolism of the temporoparietal association cortex (figure 1, A), a typical pattern for sporadic AD.[7] The patient was heterozygous for a novel insertional mutation in the *PS1* gene (see below), and no *PS1* mutations were found in his mother. Subsequent examinations revealed progressive deterioration in cognition and development of language, motor speech, and gait abnormalities. A second FDG-PET scan at age 33 showed a remarkable increase in the severity and extent of glucose hypometabolism (see figure 1, C). At his last evaluation at age 34, the patient was profoundly demented, exhibited severe dysarthria, dysphagia, and spasticity of arms and legs, and was unable to stand or ambulate unassisted.

From the Departments of Neurology (Drs. Moretti and Foster, K.J. Kluin), Pathology (Dr. Lieberman), and Psychiatry (Drs. Wilde and Giordani) and Division of Nuclear Medicine (Drs. Koeppe, Minoshima, and Kuhl), University of Michigan, Ann Arbor; and Athena Diagnostics, Inc. (Dr. Seltzer), Worchester, MA.

Dr. Moretti's current address is Department of Molecular and Human Genetics, Baylor College of Medicine, One Baylor Plaza, Rm. T836, Houston, TX 77030. Dr. Wilde's current address is Department of Physical Medicine and Rehabilitation, Baylor College of Medicine, 6560 Fannin St., Suite 1144, Box 67, Houston, TX 77030.

Supported in part by the Michigan Alzheimer's Disease Research Center (NIH grant P50-AG08671) and NIH grant RO1-NS24896. P.M. is supported by NIH NS043969-02.

Received December 5, 2003. Accepted in final form January 21, 2004.

Address correspondence and reprint requests to Dr. N.L. Foster, Department of Neurology, University of Michigan, 1920 Taubman, 1500 E. Medical Center Dr., Ann Arbor, MI 48109; e-mail: nlfoster@umich.edu

Table *Neuropsychological test results*

Cognitive domain	Case IV.3			Case IV.2, age 36
	Age 31	Age 32	Age 33	
General intellect			Impaired	
MMSE, WNL > 23	24	16	9	18
WAIS-R/III, score (percentile)				
Full-Scale IQ	69 (2nd)	60 (<1st)		63 (<1st)
Verbal IQ	76 (5th)	74 (4th)		66 (1st)
Performance IQ	64 (<1st)	50 (<1st)		65 (<1st)
Reading achievement, percentile			Impaired	
WRAT-R/AMNART	38th			62nd
Language			Impaired	
Naming, WNL ≥ 47; score (percentile)	51 (4th)	45 (<1st)		35 (<1st)
Verbal fluency, percentile	9th	4th		45th
Receptive language, percentile				33nd
Visuospatial, percentile			Impaired	
WMS (/III) copy				16th
Visual discrimination				WNL
WAIS-R/III BD	<1st	<1st		2nd
Memory			Impaired	
Memory quotient, WMS; percentile	8th	>1st		
Verbal prose recall, WMS/III; percentile				2nd
% retention	81st			57th
Verbal list learning, HVLT-R; percentile				<1st
Visual recall, WMS/III; percentile				2nd
% retention	67			23
Attention, percentile			Impaired	
Digit span, WAIS-R/III	2nd			4th
Arithmetic, WAIS-R/III	4th	4th		<1st
Executive functioning, percentile			Impaired	
Trails-Making B				<1st
WCST correct responses	3rd			12th
Motor testing, percentile			Impaired	
Strength of grip, R/L	66th/69th	27th/16th		
Tapping, R/L	21st/4th	2nd/<1st		
Manual dexterity, R/L				<1st/<1st

By age 33, Case IV.3 was too impaired to participate in the formal test measures listed here, and the Severe Impairment Battery was administered: <1–2nd percentile = impaired; 3–8th percentile = borderline impaired; 9–23rd percentile = low average; 24–75th percentile = average.

MMSE = Mini-Mental State Examination; WAIS = Wechsler Adult Intelligence Scale; WRAT = Wide Range Achievement Test; AMNART = American National Adult Reading Test; WNL = within normal limits; WMS = Wechsler Memory Scale; BD = Block Design; HVLT = Hopkins Verbal Learning Test; WCST = Wisconsin Card Sorting Test.

The proband's 36-year-old right-handed sister (IV.2) had a history of progressive memory problems, gait impairment, and slurred speech. On examination, she had a spastic gait and spasticity in all limbs, although more severe in the legs. She demonstrated mild dystonic dysarthria, verbal apraxia, prominent dysnomia, and mild stuttering. Neuropsychological testing showed significant cognitive and motor impairment relative to her estimated premorbid average abilities (see the table). Laboratory studies and brain MRI were normal, but FDG-PET demonstrated a pattern of hypometabolism similar to her brother's (see figure 1, B). She was heterozygous for the same insertional *PS1* gene mutation detected in her affected sibling.

FDG-PET scans were performed at different dementia severities (Mini-Mental State Examination [MMSE] scores of 22, 15, and 9). Hypometabolism first developed in the posterior temporoparietal cortex and later encompassed the posterior cingulate, primary motor, and frontal association cortices (see figure 1, B and C). The involvement of the primary motor cortex was apparent only after spastic paraparesis was clinically noticeable. The primary motor

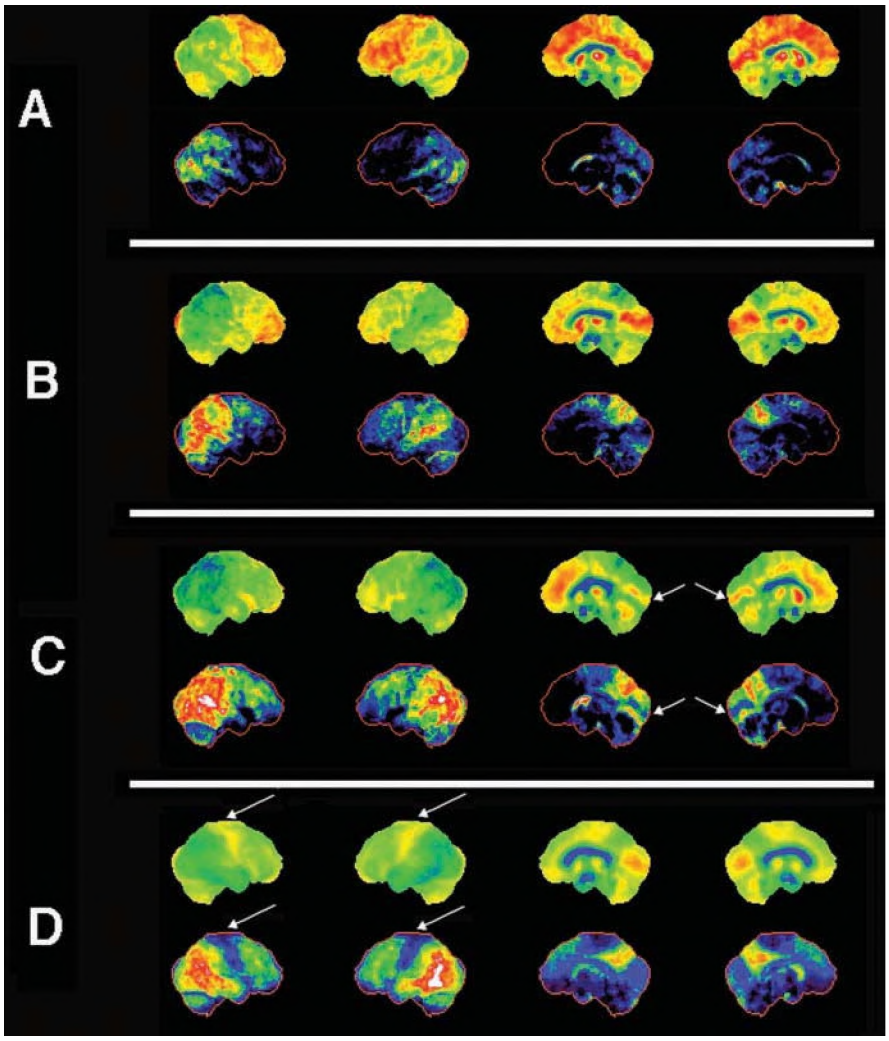

Figure 1. Cerebral glucose metabolism measured with PET following injection of 10 mCi of [^{18}F]fluorodeoxyglucose. Images show the results of three-dimensional stereotactic surface projection (SSP) analysis. Patient studies are shown in order of dementia severity at the time of study (A to C). Case IV.3 was scanned twice, when his Mini-Mental State Examination (MMSE) score was 22 (A) and again when his MMSE score was 9 (C). Case IV.2 was scanned with moderate dementia when her MMSE was 15 (B). In each panel, the four images from left to right show the right lateral, left lateral, right medial, and left medial views of the cerebral cortex. Data for each patient study are shown in two ways. The first row of each study shows cerebral glucose metabolism relative to that in the pons. Colors correspond to values of relative glucose metabolism (white > red > yellow > green > blue). The second row shows statistical SSP maps derived from pixel-by-pixel z scores where metabolism is lower in the patient than in 33 elderly normal control subjects (mean age 68 years, range 58 to 91 years). In these statistical maps, the same color scale is used, and yellow corresponds to a z score of 3. The last panel of the figure (D) shows calculated images of relative cerebral glucose metabolism for Alzheimer disease with an MMSE score of 9, comparable with the severity of the patient scanned in (C). The arrows in (C) indicate the sparing of the primary visual cortex. The arrows in (D) indicate the location of the primary motor cortex, normally spared in Alzheimer disease.

cortex of Case IV.3 exhibited the greatest change of any brain region (3.3 SD compared with normal individuals), while his MMSE declined from 22 to 9. In contrast, scans from 27 nonfamilial, autopsy-confirmed AD patients showed the greatest changes in association cortex and posterior cingulate gyrus (0.7 to 1.7 SD) as dementia severity increased from MMSE 22 to 9, with little change (0.5 SD) in the primary motor cortex. Other affected brain areas of Case IV.3 also had more rapid decline than those of typical AD subjects (1.9 to 2.7 SD), paralleling the rapid disease progression.

Gross examination of Case IV.3 revealed a 1,110-g brain with moderate atrophy primarily involving the frontal and temporal lobes. Microscopic examination showed moderate neuron loss and gliosis involving all neocortical regions, amygdala, and hippocampus. Both large eosinophilic plaques without a dense amyloid core (cotton-wool plaques)[2,8] and typical pathologic features of AD were present throughout the neocortex, limbic regions, and less severely in the striatum. No macroscopic degeneration of the corticospinal tracts was observed at the level of the midbrain. The spinal cord was not collected at the time of autopsy.

Sequencing of the *PS1* gene revealed a heterozygous 6-nucleotide insertion (TTATAT) at nucleotide position 715 of the *PS1* cDNA. This mutation is predicted to result in the substitution of tyrosine with phenylalanine and followed by the insertion of isoleucine and tyrosine, resulting in the net addition of phenylalanine and isoleucine between codons 156 and 157.

Discussion. Previously reported *PS1* mutations causing AD are due to missense mutations, with rare examples of genomic deletions or insertions of single amino acids due to splice site mutations.[1,2,9] The mutation in our pedigree is novel because it is a genomic insertion of 6 nucleotides and is located in the region of exon 3 encoding the intracellular loop between transmembrane domains 2 and 3 of PS1. This region shares significant homology in both PS1 and PS2 and is highly conserved phylogenetically, suggesting it may have a critical function.

The physiologic implications of this mutation are not fully understood. However, several features suggest that this novel mutation causes an unusually aggressive form of AD: 1) the early age at onset, severity, and rapid progression of neurologic and

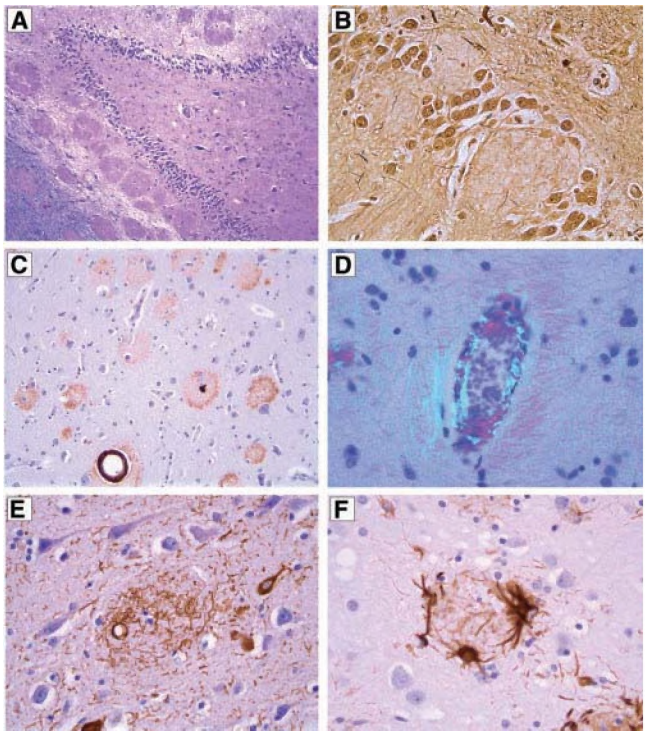

Figure 2. Cotton-wool plaques in familial Alzheimer disease, Case IV.3. (A) Round, eosinophilic cotton-wool plaques in the hippocampus. Luxol fast blue/cresyl violet/eosin; ×200. (B) Cotton-wool plaques in the dentate gyrus, displacing normal structures. These plaques have a distinct central pallor on Bielschowsky silver stain. ×400. (C) Immunohistochemical stain for β-amyloid protein highlights cotton-wool plaques and shows a uniform to peripherally accentuated distribution. Less frequent classic neuritic plaques are also present and contain a densely stained amyloid core. A blood vessel whose wall is immunoreactive for β-amyloid protein is present at the bottom of the field. ×200. (D) Amyloid deposition in blood vessel wall is highlighted by birefringence in polarized light after Congo red stain. ×400. (E) Immunohistochemical stain for tau reveals uniformly distributed threads throughout the cotton-wool plaque. Adjacent neurons contain neurofibrillary tangles. ×400. (F) Reactive astrocytes located at the periphery of cotton-wool plaques. Glial fibrillary acidic protein immunohistochemistry; ×400.

neuropsychological deficits; 2) the development of spastic paraparesis, dystonia, and motor speech changes unexpected in AD; 3) the pathologic involvement of both cortical and subcortical structures to an unusual degree; and 4) the more rapid progression and wider topographic extent of hypometabolism seen by FDG-PET as compared with typical AD.

The patients' initial cognitive deficits reflected a severity typically seen only after several years of progression of AD, and Case IV.3 had more than twice the mean rate of expected cognitive decline.[10] The early development of spastic paraparesis, dystonia of the upper extremities, and dysarthria with dystonic components indicated a widespread dysfunction of the motor system that was confirmed with FDG-PET scans and neuropathology. Glucose hypometabolism of the primary motor–sensory cortex was much greater than in equally demented typical patients with AD[6] (see figure 1, D, arrows). Cotton-wool plaques and large eosinophilic β-amyloid plaques lacking congophilia and with little associated neuritic pathology[2,8] were present in all sections of the neocortex including the motor cortex (figure 2). These plaques have been described in some cases of AD with spastic paraparesis and have been proposed to be associated with more aggressive *PS1* mutations. Fewer plaques and less severe gliosis also were noted in the basal ganglia.

Although pathology in this pedigree is more widespread than typical, there is also evidence that the usual regional hierarchy of disease pathology is preserved, with initial damage of memory systems and association cortex. FDG-PET showed predominant temporoparietal hypometabolism expected in sporadic AD.[7] Like typical patients with AD and unlike other disorders like HSP, our subjects developed cognitive problems first, although attention later easily was diverted to obvious motor symptoms. As a consequence, this novel insertional *PS1* mutation is a good model for AD, exhibiting an accelerated rate of disease progression and more extensive topographic distribution of pathology.

Acknowledgment

The data were obtained in the course of clinical care and as part of research studies approved by the University of Michigan Institutional Review Board. They are used with the written permission of the subjects. The authors thank the family members and their physicians for their participation. They also thank Laurie Bluemlein and Kris Wernette for support in the care of this family and Virginia Rogers and Leslie Botti for assistance in analysis of the FDG-PET images.

References

1. Kwok JB, Taddei K, Hallupp M, et al. Two novel (M233T and R278T) presenilin-1 mutations in early-onset Alzheimer's disease pedigrees and preliminary evidence for association of presenilin-1 mutations with a novel phenotype. Neuroreport 1997;8:1537–1542.
2. Crook R, Verkkoniemi A, Perez-Tur J, et al. A variant of Alzheimer's disease with spastic paraparesis and unusual plaques due to deletion of exon 9 of presenilin 1. Nat Med 1998;4:452–455.
3. Barrett A. A case of Alzheimer's disease with unusual neurological disturbances. J Nerv Ment Dis 1913;4:361–374.
4. Ishii K, Willoch F, Minoshima S, et al. Statistical brain mapping of 18F-FDG PET in Alzheimer's disease: validation of anatomic standardization for atrophied brains. J Nucl Med 2001;42:548–557.
5. Minoshima S, Frey KA, Koeppe RA, Foster NL, Kuhl DE. A diagnostic approach in Alzheimer's disease using three-dimensional stereotactic surface projections of fluorine-18-FDG PET. J Nucl Med 1995;36:1238–1248.
6. Minoshima S, Giordani B, Berent S, et al. Metabolic reduction in the posterior cingulate cortex in very early Alzheimer's disease. Ann Neurol 1997;42:85–94.
7. Foster NL, Chase TN, Fedio P, et al. Alzheimer's disease: focal cortical changes shown by positron emission tomography. Neurology 1983;33:961–965.
8. Verkkoniemi A, Kalimo H, Paetau A, et al. Variant Alzheimer disease with spastic paraparesis: neuropathological phenotype. J Neuropathol Exp Neurol 2001;60:483–492.
9. Rogaeva E, Bergeron C, Sato C, et al. PS1 Alzheimer's disease family with spastic paraplegia: the search for a gene modifier. Neurology 2003;61:1005–1007.
10. Salmon DP, Thal LJ, Butters N, Heindel WC. Longitudinal evaluation of dementia of the Alzheimer type: a comparison of three standardized mental status examinations. Neurology 1990;40:1225–1230.